

CFD-Based Numerical Method for Temperature Set-Point Commissioning and PMV Assessment of Occupied Individual Air-Conditioning Zone



Xiang Deng, Xue Xue  and Bugong Xu

Abstract Traditional air-conditioning control system assumes indoor air temperature to be uniformly distributed. However, indoor air is often not completely well-mixed. The air temperature and speed data obtained from sensors cannot represent thermal state of the whole room. This paper aims to investigate real thermal perception of the occupants in an air-conditioned office model. A Computational Fluid Dynamics (CFD) based method is utilised for building modelling. The temperature and air speed calibrations are adopted to offset the temperature and air speed difference between the actual sensors (i.e. temperature and speed sensors) and the virtual sensors (i.e. temperature and speed sensors) located in the occupied zone. Predicted Mean Vote (PMV) method is employed to evaluate the thermal comfort performance under different indoor air conditions. Simulation results show that indoor thermal comfort performance in a specified office model is well improved by calibrating the differences between the actual and virtual temperature sensors.

Keywords Computational fluid dynamics · Control commissioning · Predicted mean vote · Air-conditioning · Temperature setpoint

1 Introduction

Since people averagely spend more than 90% of their time in buildings, it is critical to ensure a satisfactory indoor environment [1]. For air-conditioned buildings, well-designed air-conditioning system could increase indoor thermal comfort while

X. Deng · B. Xu
School of Automation Science and Engineering, South China University of Technology,
Guangzhou, China

X. Deng · X. Xue (✉)
Research and Development Centre, Shenzhen DAS Intellitech Co., Ltd., Shenzhen, China
e-mail: xuexue@hanergy.com

minimising building energy consumption [2]. Over the last decades, many works [3–6] have been devoted to the development of indoor thermal comfort when using air conditioning. These studies suggested that by no means could the indoor air be perfectly mixed and create an even thermal and air speed field in an air-conditioned space. In addition, it is not generally necessary to ensure the overall thermal comfort performance of the whole space. The primary focus should naturally be on occupied areas where local thermal discomfort caused by temperature and air velocity variations and building interior layout could influence thermal satisfaction of the occupants significantly. The air-conditioning system should be operated based on calibrated air temperature and speed which could represent the thermal state of the place of interests.

This paper investigates the thermal perception of the occupants in the occupied zone of an air-conditioned office model. CFD is employed to analyse temperature and air speed in the occupied zone. A space temperature offset model is developed to offset the difference in air temperatures. Based on the calibrated temperature, temperature set-point in the building model is commissioned to cater to the Predicted Mean Vote (PMV) requirement at the place of interests to improve occupant thermal comfort.

2 Methods

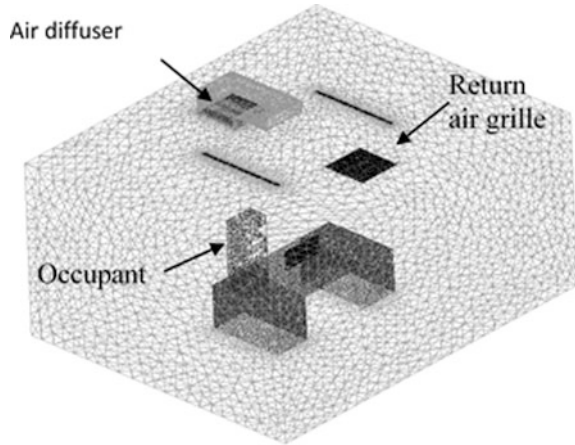
2.1 Case Study Room Model

Field measurements are reliable for IEQ evaluation IEQ but time-consuming and labour-costing. Hence, CFD simulation as an alternative is used to represent the room. As highly detailed CFD models would not greatly improve the accuracy of simulation results but significantly increase simulation time, the building model should be simplified but with the main building air flow characteristics captured [7]. The detailed introduction of the room model selected for this study (Fig. 1) is explained as follows.

The building model of dimensions $5 \times 4 \times 3 \text{ m}^3$ ($L \times W \times H$) was an air-conditioned room. No-slip and no penetration boundary conditions were implemented for all the room surfaces. The facade was assumed to be a glass wall with a constant radiation heat flux of 50 w/m^2 while that of other walls was set as 30 w/m^2 ; the floor and ceiling were presumed to be adiabatic [8]. Since the diminished effect of the flow resistance caused by the indoor furniture could not be ignored [9], a table was placed in the middle of the room and a cube of $0.4 \times 0.24 \times 1.2 \text{ m}^3$ ($L \times W \times H$) was established by the table to approximately represent a seated person. The table was presumed to be adiabatic. The heat generation rates of the occupant and laptop on the table were 65 and 20 w.

A mesh of approximately 326,000 cells was utilised for the CFD computation after making a trade-off between model accuracy and computation cost. ANSYS Fluent program was utilised for the indoor and outdoor airflows simulation by using

Fig. 1 A schematic view of the room model



Reynolds averaged Navier–Stokes (RANS) equations with standard $k - \varepsilon$ turbulence modelling [10]. Convergence was assumed to be obtained when a minimum of 1×10^{-4} was reached for the residuals of continuity, momentum, turbulent kinetic energy and its dissipation rate and 1×10^{-7} for the residual of energy [8].

The supply air flow speed in the supply air duct near the air diffuser was set to be 2–7 m/s with an interval of 1 m/s. The supply air flow temperature was adjusted from 12 to 18 °C with an interval of 0.5 °C. The actual temperature was presumed to be placed in the return air grille and a virtual sensor was placed in occupied zone. Based on the CFD simulation, the temperature difference between virtual and actual sensors and the local air speed in the occupied zone could be obtained.

2.2 Thermal Comfort Performance Assessment

The PMV model proposed by Fanger [11] was used for indoor thermal comfort evaluation. The model includes the six variables influencing the thermal sensation of occupants. The values of these variables were chosen from the literature [12–14] for buildings in the subtropical area of China for a typical summer day (Table 1).

Table 1 Parameter values assumed

Metabolic rate (W/m^2)	Clothing insulation (Clo)	Air temperature ($^{\circ}C$)	Wall/floor/ceiling temperature ($^{\circ}C$)	Air speed (m/s)	Relative humidity (%)
65	0.5/0.7	Simulated values	24	Simulated values	60

PMV was post-processed using the User Defined Function (UDF) in the ANSYS Fluent. A thermal comfort performance contour map based on PMV was constructed under different air temperatures and air speeds in the occupied zone. A PMV value of 0 was defined to be thermal neutrality [15]. By use of the thermal neutrality line (i.e. $PMV = 0$) in the thermal comfort performance contour map, a synchronisation adjustment to supply air speed can be made when the temperature set-point in the occupied zone is commissioned.

2.3 Temperature Set-Point Commissioning

The thermal neutrality line in the thermal performance contour map provided a series of temperature set-points with corresponding air speeds. The variable static pressure and temperature (VPT) control method [16] which is normally employed by air handling unit (AHU) to adjust the supply air temperature and speed/flow rate could be used to maintain thermal neutrality in the occupied zone.

TRNSYS was used as the simulation platform to examine the performance of the VPT control strategy based on the thermal neutrality line which is obtained from CFD simulations. A simplified AHU model originally derived from YORK YAH03A AHU was developed in TRNSYS program (see Fig. 2) to provide mixed cooling air for the case study room model.

3 Results

3.1 Air Speed Profile

An example of the air speed profile (supply speed of 7 m/s) is presented in Fig. 3.

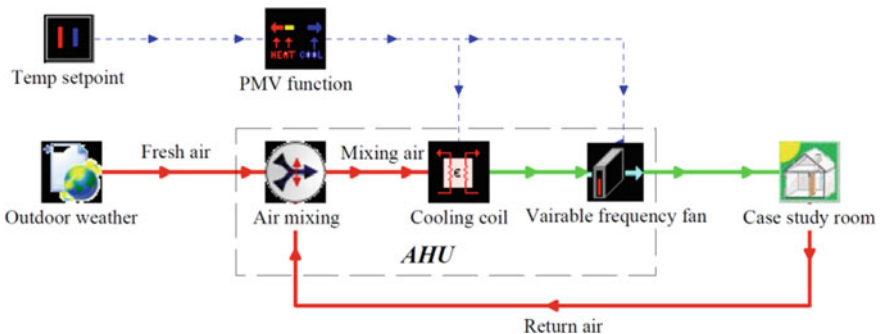


Fig. 2 Schematic of VPT control based on thermal neutrality

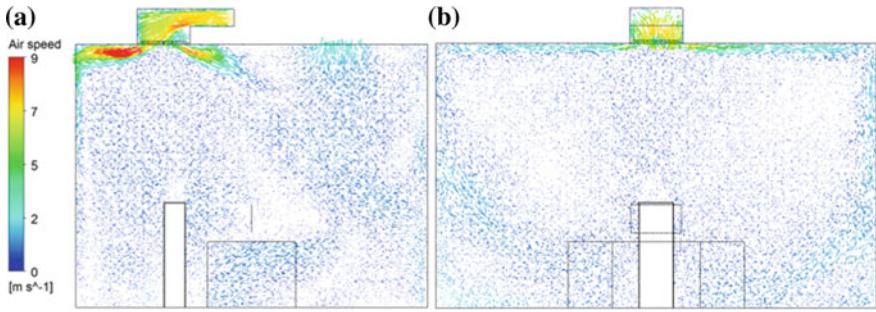


Fig. 3 Velocity field: **a** lateral view; and **b** elevation view

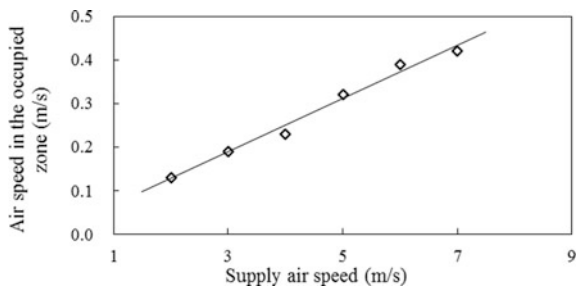
Airflow from air duct spread to surrounding with a relatively high speed as a result of the diffuser. The main fraction of the airflow moved forward along the surface of the ceiling and then went downward due to Coanda Effect [17]. The distribution of airflow speed was comparatively uniform in the bottom of the case study room model and no jet flow directly entered the occupied zone. The relations between air speed in the occupied zone and the supply air speed was summarised in Fig. 4.

The air speed in the occupied zone increases linearly with supply air speed. A maximum air speed associated with 0.42 m/s in the occupied zone was obtained when the supply air speed was 7 m/s.

3.2 Temperature Offset

When the airflow and temperature fields in the case study room came to steady, the temperatures in the occupied zone and the return air grille could be obtained. Figure 5 presents the temperature difference between virtual and actual sensors when the supply air temperature varies from 12 to 18 °C with a supply air speed of

Fig. 4 Air speed in the occupied zone



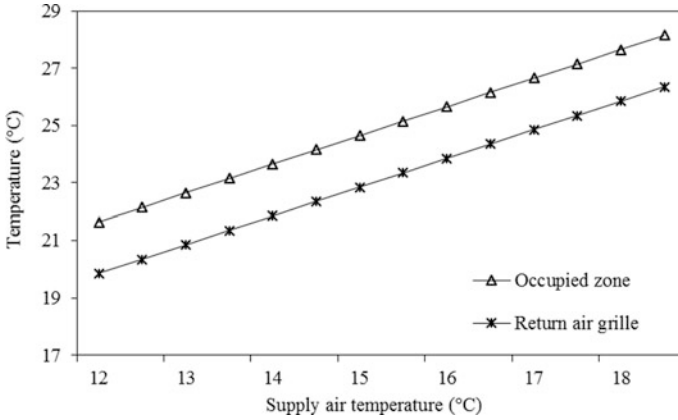


Fig. 5 Temperatures in the occupied zone and return air grille

5 m/s. With the increase of supply air temperature, temperatures in occupied zone and return air grille raised linearly. Meanwhile, the temperature difference between actual and virtual sensors decreased with the increasing supply air flow speed. Figure 6 reveals the relations between temperature difference and supply air speed.

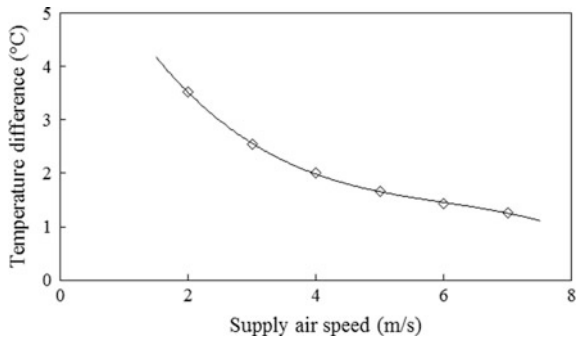
According to Fig. 6, virtual sensor temperature (T_v) as a function of the supply air speed (V_{sup}) and actual sensor temperature (T_a) could be regressed:

$$T_v = 0.094 * V_{sup}^2 - 1.276 * V_{sup} + 5.632 + T_a \tag{1}$$

3.3 Thermal Comfort Performance Contour Map

Thermal comfort performance based on PMV index could be obtained under different supply air speeds and temperatures in the occupied zone. Figure 7

Fig. 6 Temperature difference between virtual and actual sensors



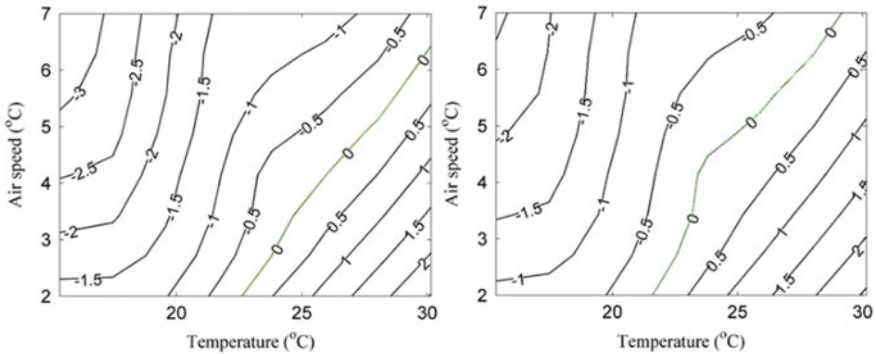


Fig. 7 Contour maps of the PMV index: **a** clo = 0.5; and **b** clo = 0.7

demonstrates the performance contour maps when cloth insulations were selected as 0.5 and 0.7.

Thermal neutrality (i.e. PMV = 0) lines are highlighted in Fig. 7. The lines showed that the minimum temperature in the occupied zone to achieve thermal neutrality was 22 °C for clo = 0.5 and 23 °C for clo = 0.7 (associated with the actual sensor temperature of 18.5 and 19.5 °C) and the corresponding supply air speed was then adjusted as 2 m/s. The maximum temperature could be as high as 29 °C (associated with the actual sensor temperature of 25.5 °C) for both two scenarios when the supply air speed reached 7 m/s, indicating the influence of cloth insulation on thermal comfort diminished with the increase of supply air speed in the specified conditions in this study.

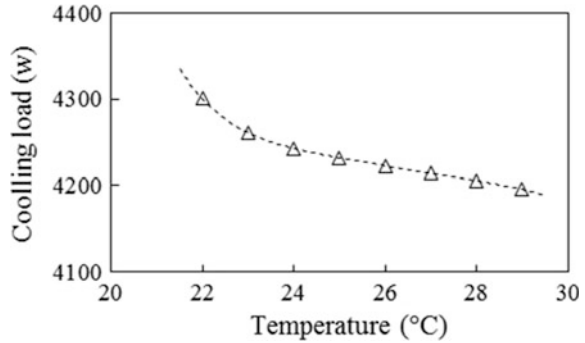
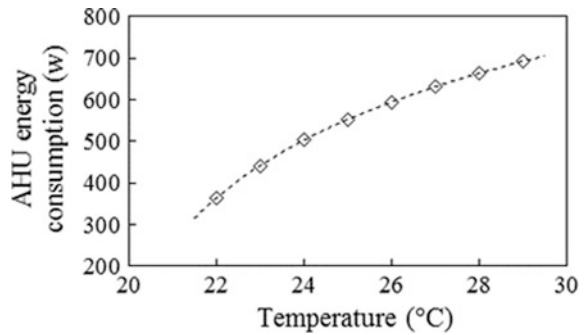
3.4 Temperature Set-Point Commissioning

Thermal neutrality line in Fig. 7a (i.e. the cloth insulations were 0.5) was used for temperature set-point commissioning. Figures 8 and 9 illustrate the TRNSYS simulated results of average cooling loads and AHU energy consumptions under different temperature set-point during a whole typical summer workday in Shenzhen, China.

When raising the temperature set-point, the cooling demand for handling the mixing air decreased; however, to ensure the thermal comfort requirement of the occupants, the airflow rate had to be increased by uprating fan operating frequency which would increase the AHU energy consumption.

Figure 9 displays the overall energy consumptions by chiller and AHU when temperature set-point varies. The coefficient of performance (COP) for the chiller was assumed to be 3 as a constant value.

According to Fig. 10, overall energy consumption has a positive correlation with the temperature set-point. Therefore, for the specified conditions given in this study,

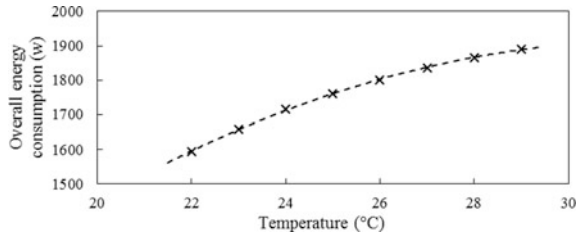
Fig. 8 Cooling load**Fig. 9** AHU energy consumption

the optimal temperature in the occupied area to achieve thermal neutrality while minimising the energy consumption of the HVAC system (Chiller + AHU) could be identified as 22 °C.

4 Discussion

As the maximum acceptable air speed for occupants in an air-conditioned room was suggested to be 0.8 m/s according to ASHRAE 55 [14], the gentle and steady flow (see Fig. 3) in the occupied zone of the case study room model did not bring any draught risks; regardless of the supply air temperature, the temperature difference between virtual and actual sensors was kept invariable (i.e. 1.8 °C with a supply air speed of 5 m/s in Fig. 5) due to the fact that the heat generated in the room was assumed to be constant; the theoretical optimal temperature value for this case study room was identified based on the hypothesis of a constant COP value. The overall energy consumption line in Fig. 10 remains to be identified with variable COP values in practice and the optimal temperature might differ from the theoretical one; this study is restricted to numerical simulation analysis. Therefore, field study based

Fig. 10 Overall energy consumption



on practical air-conditioned buildings should be performed to conduct a temperature set-point commissioning based global optimisation for the whole HVAC energy consumption in the future.

5 Conclusions

A thermal neutrality based indoor thermal comfort control method was presented by integrating a CFD room model into its air-conditioning system in TRNSYS to evaluate the thermal comfort and energy consumption performances. The temperature compensation between the return air and air in the occupied zone was determined by regressing a temperature offset function. Thermal neutrality lines were identified in the thermal comfort performance contour maps. Through temperature set-point commissioning, the optimal temperature in the occupied zone was figured out to achieve thermal comfort and energy conservation. Despite its preliminary character, this research provided a novel method to commission temperature set-point in buildings to improve thermal comfort in the occupied individual area and reduce HVAC energy consumption.

References

1. Prakash, D.: Transient analysis and improvement of indoor thermal comfort for an air-conditioned room with thermal insulations. *Ain Shams Eng. J.* **6**(3), 947–956 (2015)
2. Zhang, W., Liu, F., Fan, R.: Improved thermal comfort modeling for smart buildings: a data analytics study. *Int. J. Electr. Power Energy Syst.* **103**, 634–643 (2018)
3. Aryal, P., Leephakpreeda, T.: CFD analysis on thermal comfort and energy consumption effected by partitions in air-conditioned building. *Energy Procedia* **79**, 183–188 (2015)
4. Buratti, C., Palladino, D., Moretti, E.: Prediction of indoor conditions and thermal comfort using cfd simulations: a case study based on experimental data. *Energy Procedia* **126**, 115–122 (2017)
5. Zheng, C., You, S., Zhang, H.: Comparison of air-conditioning systems with bottom-supply and side-supply modes in a typical office room. *Appl. Energy* **227**, 304–311 (2018)
6. Gilani, S., Montazeri, H., Blocken, B.: CFD simulation of stratified indoor environment in displacement ventilation: validation and sensitivity analysis. *Build. Environ.* **95**, 299–313 (2016)

7. Hutmacher, D.W., Singh, H.: Computational fluid dynamics for improved bioreactor design and 3D culture. *Trends Biotechnol.* **26**(4), 166–172 (2008)
8. Sun, Z., Wang, S.: A CFD-based test method for control of indoor environment and space ventilation. *Build. Environ.* **45**(6), 1441–1447 (2010)
9. Bojic, M., Yik, F., Lo, T.Y.: Locating air-conditioners and furniture inside residential flats to obtain good thermal comfort. *Energy Build.* **34**(7), 745–751 (2002)
10. Chen, Q.: Comparison of different $k - \epsilon$ models for indoor air flow computations. *Numer. Heat Transf. Part B: Fundam.* **28**(3), 353–369 (1995)
11. Fanger, P.O.: *Thermal Comfort. Analysis and Applications in Environmental Engineering.* Danish Technical Press, Copenhagen (1970)
12. De Dear, R., Leow, K., Foo, S.: Thermal comfort in the humid tropics: field experiments in air conditioned and naturally ventilated buildings in Singapore. *Int. J. Biometeorol.* **34**(4), 259–265 (1991)
13. De Dear, R., Brager, G.S.: Thermal comfort in naturally ventilated buildings: revisions to ASHRAE Standard 55. *Energy Build.* **34**(6), 549–561 (2002)
14. Standard, ASHRAE: Standard 55-2013. *Thermal Environmental Conditions for Human Occupancy* (2013)
15. ISO E: 7730: 2005. *Ergonomics of the Thermal Environment. Analytical Determination and Interpretation of Thermal Comfort Using Calculation of the PMV and PPD Indices and Local Thermal Comfort Criteria* (2006)
16. Li, K., Ye, D.: VPT control and its application in VAV air conditioning systems. *HV&AC29* (3):7–10 (1999)
17. Jiang, M., Law, A.: Mixing of swirling inclined dense jets—a numerical study. *J. Hydro-Environ. Res.* **21**, 118–130 (2018)